THE ASTROPHYSICAL JOURNAL, 356:119–129, 1990 June 10

TWO VARIABLE X-RAY SOURCES IN M31

A. COLLURA
Istituto per le Applicazioni Interdisciplinari della Fisica, Palermo
AND
F. REALE AND G. PERES
Osservatorio Astronomico di Palermo
Received 1988 December 27; accepted 1989 December 12

ABSTRACT

We have analyzed the entire set of *Einstein* observations of M31, consisting of five imaging proportional counter and nine high resolution imager observations, for variability of the X-ray sources. The time scales explored range up to $\sim 10^5$ s, the maximum time span of individual observations. We detect variability above the adopted 99.73% significance level in two sources and derive constraints on their possible periodicity.

The observed X-ray luminosities, the pattern of variability, and the optical identifications suggest the possibility that one of them is a low-mass X-ray binary and the other one a compact massive X-ray binary.

We also discuss the analysis of the nonvariable sources and derive upper limits on the detectable variability of the various sources. The number of variable sources detected is in agreement with the expectations based on the features of intense Galactic X-ray sources and on the characteristics of the observations.

Subject headings: galaxies: individual (M31) — X-rays: binaries — X-rays: sources

I. INTRODUCTION

M31, the nearest large spiral galaxy, is among the best studied extragalactic objects. It was a target of primary interest for the X-ray *Einstein* telescope (Giacconi *et al.* 1979), being an unexcelled laboratory for a large variety of studies, including morphological comparisons with our Galaxy and detailed analysis of X-ray sources. *Einstein* observations of M31 have been the object of previous work: van Speybroeck *et al.* (1979) made a first analysis of the observations, obtaining some optical identifications of the X-ray sources; Fabbiano, Trinchieri, and van Speybroeck (1987) studied the X-ray spectral properties of the bulge of M31; Crampton *et al.* (1984), henceforth C84, pursued the optical identification of the individual X-ray sources in M31 and found that most of them could be classified in three categories of objects: blue stars, globular clusters, and supernova remnants. Some of the identifications are, however, quite uncertain, and additional information could clarify the nature of the X-ray sources. In this respect, it is worthwhile to study their variability because it provides unique information on the nature of the sources.

Analogously, Peres *et al.* (1989) analyzed the variability of the X-ray sources of M33. They identified one of the sources with an X-ray eclipsing binary and confirmed the active nature of the nucleus of M33. These results proved the feasibility and the effectiveness of studies of variability even of nonnuclear extragalactic X-ray sources, thanks to the high sensitivity of the *Einstein* satellite.

In this paper we present a systematic variability analysis of the M31 X-ray sources observed by *Einstein.* We mainly focus on variations on time scales within individual observations, i.e., $\lesssim 10^5$ s. The expectation of such a work is to detect variability from the most intense and variable X-ray sources of a galaxy, i.e., nuclear sources and binary systems containing a compact source. In § II we present the data and describe the method of analysis; in § III we present our results; in § IV we discuss our findings and draw our conclusions.

II. DATA AND ANALYSIS

The data analyzed in this work were collected with the *Einstein Observatory* and consist of five observations done with the imaging proportional counter (IPC) and nine with the high resolution imager (HRI). In Table 1 we provide, for each observation, the identification number (preceded by H or I for HRI and IPC observations, respectively), the date and time of start, the date and time of end, the net observation time, and the mean background in the field. Each observation typically consists of a sequence of continuous exposures, separated by gaps due to several technical reasons. Two HRI observations, H4483 and H4486, in addition undergo an interruption lasting several months, and therefore each of them will be considered as two different observations. The fields observed cover the whole extension of M31 ($\sim 3°$) and overlap only partially (van Speybroeck *et al.* 1979). In Figures 1*a* and 1*b* we show the fields of view of the IPC and HRI observations, along with all of the detections of the X-ray sources obtained with the Final Data Processing of the *Einstein* data (Harnden *et al.* 1984, 1989).

The preliminary data reduction, including source detection, was done with the abovementioned processing system. Variability analysis was performed on the arrival times of photons detected within a radius of 3′ from the source position, for IPC observations, and a radius of 6″.75 for HRI observations. We selected only the detections yielding at least 60 counts, a threshold corresponding to the applicability limit of the method of variability analysis chosen (Collura *et al.* 1987). All of the detections close to the support structure or edges of the detector window were excluded from the sample because the jitter of the telescope pointing could artificially modulate the photon flux. We take into account only the sources found with the *local detection method* (Harnden *et al.* 1984). We discarded IPC observation I573 because the pointing was unstable to such an extent that we could no longer correct for the influence of the edges and supporting structure of the window, or for the influence of the spatial changes of the detector gain with

TABLE 1

OBSERVATIONS

Sequence No.	Start Time (UT)	Stop Time (UT)	Net Time (s)	Background[a] Soft	Background[a] Hard	Background[a] Total
I574	1979-01-11 00:12:41.8	1979-01-11 20:21:01.0	35383.3	271	366	589
I575	1979-01-11 20:24:25.8	1979-01-12 17:00:03.4	31668.2	212	218	426
H579	1979-01-13 16:56:23.2	1979-01-14 08:30:57.1	28031.5	...	...	8
I573	1979-01-23 03:43:17.9	1979-01-23 23:46:09.5	20434.6	109	127	232
I4490	1979-08-02 08:43:55.9	1979-08-02 16:01:31.3	10695.8	71	97	144
H4479	1979-08-04 07:18:05.2	1979-08-05 10:44:40.7	25563.9	...	...	7
H4480	1979-08-05 18:09:05.7	1979-08-06 21:35:41.2	26499.5	...	...	5
H4481	1979-08-07 05:40:22.8	1979-08-07 10:10:43.0	9419.8	...	...	2
H4484	1979-08-07 17:00:19.0	1979-08-07 21:10:40.9	9812.5	...	...	2
H4486[b]	1979-08-07 21:20:24.7	1979-08-08 05:07:16.6	15631.0	...	...	7
	1980-01-16 03:32:35.3	1980-01-16 18:51:44.9	14092.5			
H4485	1979-08-08 05:09:24.2	1979-08-08 20:59:40.6	24309.9	...	...	5
H4483[b]	1979-08-08 12:55:39.9	1979-08-08 23:55:08.4	12228.6	...	...	7
	1980-01-13 17:05:41.4	1980-01-14 21:19:43.0	16859.4			
H7066	1980-01-13 14:56:59.8	1980-01-14 16:39:38.4	10054.3	...	...	4
I5021	1980-07-28 19:18:32.9	1980-07-28 23:09:58.3	7757.5	38	43	79

[a] This is the number of background counts expected, in average, in the source cell used for the variability analysis. It is based on the mean field background. The background of the HRI is obtained in the whole 0.15–3.5 keV passband.

[b] This sequence number identifies two sections of the same observation taken a few months apart. Information for each section is reported separately in two contiguous lines.

acceptable uncertainties. In fact, in Figure 1*a* some of the sources thereby detected are outside the nominal field of view. According to the above criteria, we selected a total of 21 HRI and 38 IPC detections.

Tables 2, 3, and 4 report the cross identifications among the detections selected for variability analysis in the different observations. Table 2 provides the identification number of each source, followed by an I to denote IPC sources, all of the sequences in which it was detected, the number identifying the detection within that sequence, the corresponding coordinates, and the identification either provided by C84 or imposed by us, with the procedure explained in § IV*d*. IPC *detections* in different observations are considered as the same *source* if closer than 1′. Analogously Table 3 reports the cross identifications of the HRI detections, assumed to be the same source if closer than 10″. We note that the matching criteria used are not critical. In particular, using 2′ instead of 1′ for the IPC would introduce an ambiguity in the match only of one source. As for

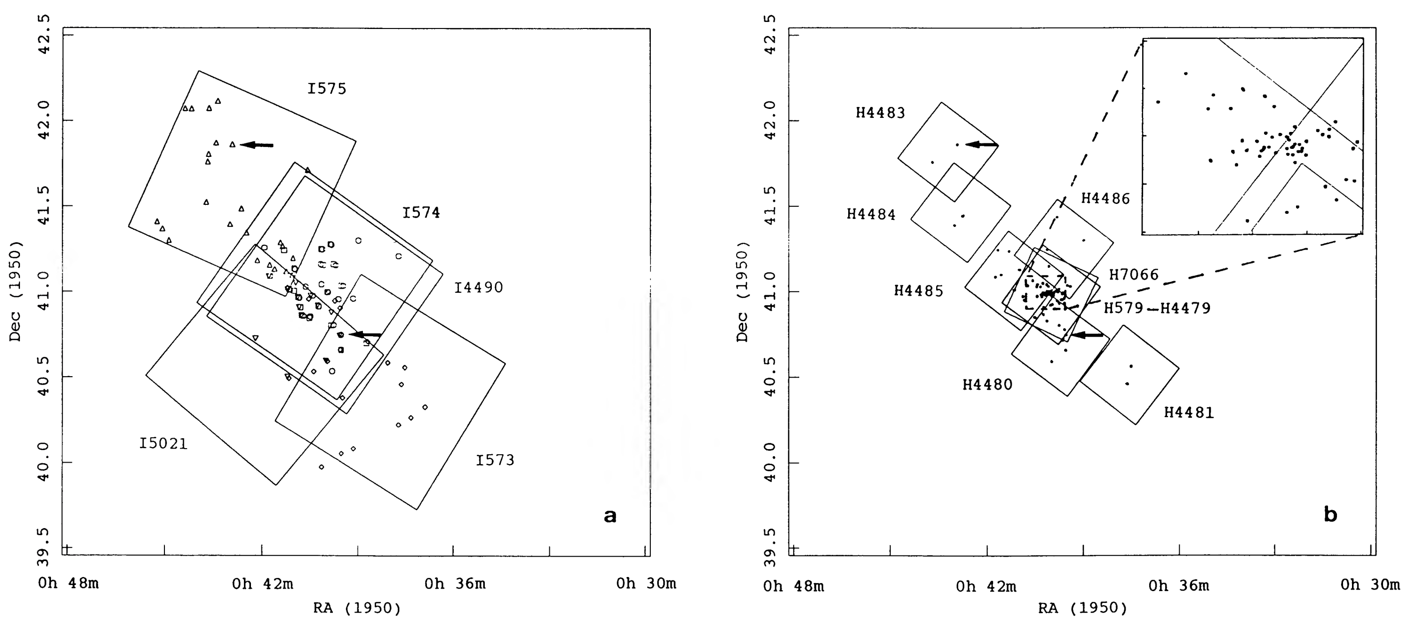

FIG. 1.—Sky map showing the fields observed by the IPC (*a*) and the HRI (*b*) with all the sources detected and reported by the standard data analysis. We have analyzed for variability only those detections yielding at least 60 counts (cf. § II). (*Triangles*: I575; *circles*: I574; *squares*: I4490; *inverted triangles*: I5021; *diamonds*: I573). In panel (*a*) the radius of the circle circumscribed to each symbol is 1′, i.e. equal to the typical IPC error on position determination. The detections of sources of I573 just outside the nominal field of view are due to the drift of the pointing during the observation; the whole observation was not included in our analysis (see text for the rejection of these data). In panel (*b*) the zoomed image in the upper right side includes the nuclear region and its surroundings. The symbol size is indicative of the error on the position only in the zoomed part of the image but, for graphical convenience, much larger in the rest of the image. The arrows point to two sources found variable (see § III).

TABLE 2

IPC–IPC Cross Identifications

Source	Sequence No.	Detection No.[a]	α(1950)	δ(1950)	Type[b]
1I	I574	1	$0^h37^m42\overset{s}{.}4$	41°12′36″	F
2I	I574	3	0 39 8.2	40 57 38	F
3I	I574	4	0 39 27.6	41 2 1	F
	I4490	3	0 39 31.8	41 2 3	
4I[c]	I574	5	0 39 31.3	40 44 51	G
	I5021	1	0 39 34.6	40 44 40	
5I	I574	6	0 39 31.9	40 39 35	NI
6I	I574	7	0 39 36.6	40 57 22	NI
7I	I4490	4	0 39 45.6	41 9 36	NI
8I	I574	9	0 39 45.5	40 48 14	NI
9I	I574	11	0 39 49.9	41 16 24	G
	I4490	6	0 39 52.0	41 16 37	
10I	I574	12	0 39 56.5	40 59 47	x
	I4490	7	0 39 57.9	40 59 55	
11I	I574	13	0 40 7.1	41 14 50	G
	I4490	9	0 40 9.2	41 14 56	
12I	I574	14	0 40 8.6	41 2 32	y
13I	I574	15	0 40 10.0	41 9 34	z
	I4490	8	0 40 5.8	41 9 19	
14I	I574	16	0 40 13.5	40 54 49	B
	I4490	10	0 40 14.3	40 54 50	
15I	I574	17	0 40 24.7	40 58 34	G
16I	I574	18	0 40 29.4	40 51 11	G
	I4490	11	0 40 31.1	40 50 43	
17I	I574	19	0 40 38.8	41 1 47	B
18I	I574	20	0 40 42.8	40 51 24	B
	I4490	12	0 40 46.1	40 51 45	
19I	I574	21	0 40 50.2	40 57 46	G
	I4490	14	0 40 52.1	40 58 3	
	I5021	8	0 40 53.5	40 58 0	
20I	I4490	15	0 40 59.6	41 0 17	y
21I	I4490	16	0 40 59.8	41 8 9	B
22I	I574	23	0 41 7.9	41 0 31	B
	I4490	17	0 41 9.9	41 0 53	
	I5021	11	0 41 12.7	41 0 49	
23I	I4490	18	0 41 19.0	41 14 31	G
24I	I4490	19	0 41 45.2	41 5 28	G
25I[c]	I575	13	0 42 54.3	41 51 43	B

[a] This is the identification number of the detection within the observing sequence as provided by the final standard data processing.

[b] The source types are blue star (B); globular cluster (G); foreground candidate (F); not identified by C84 (NI); not detected by C84 but statistically classified as foreground star through Monte Carlo method (x); not detected by C84 but statistically classified as low mass X-ray binary through Monte Carlo method (y); not detected by C84 but statistically classified as massive X-ray binary through Monte Carlo method (z). Note that the statistical classifications are artificial, do not represent a real identification of these sources, and are used only for computing the expected number of variability detections.

[c] This detection shows variability.

the HRI matches, we note that 10″ is a conservative distance, because all of the sources cross-identified by us are indeed closer than 3″. In Table 4 we report the list of HRI sources falling within 3′ from any IPC source and matching our selection criteria. The size of the cell used in the timing analysis of the IPC sources is 3′. An unequivocal cross identification between detections of the two instruments is difficult because of the moderate spatial resolution of the IPC ($\sim 1'$) with respect to the HRI ($\sim 3''$) and because of the large number and the high density of sources detected in some fields.

We have adopted a significance threshold of 99.73% for detection of variability in each energy band (see below) of each individual source detection analyzed. Individual observations have been analyzed with a modified version developed by Collura *et al.* (1987) of the classical χ^2 test, henceforth "$\bar{\chi}^2$ method." It yields results independent of any particular binning of data, since it samples several sizes and phases of the bins compatibly with the data statistics. The significance of variability obtained takes into account all of the binning sizes and phases explored in the analysis. The time scale and the effective amplitude of the variability are derived assuming that the emission arises from a constant component plus a sequence of randomly spaced, square-shaped pulses of equal amplitude and equal duration. The time scale is the duration of an individual pulse and is uncertain by a factor ~ 2 for variability at the 99.73% significance level; the uncertainty decreases steadily for higher significance (see Collura *et al.* [1987] for further details). In the presence of periodic variability, characterized by alternating "on" and "off" states, the time scale derived is the mean duration of "on" states or "off" states, whichever has the shortest duty cycle, and hence it is not necessarily related to the period. The effective amplitude $V_{\rm eff}$ is related to the pulse amplitude V_0 by the equation $V_{\rm eff}(\Delta t < \tau) = V_0 \times [\delta(1-\delta)]^{1/2}$, where τ is the pulse width and δ is the duty cycle of the variable component. For the case of a sinusoidal variability, formula [3.5] of Collura *et al.* (1987) is more appropriate; it yields

TABLE 3

HRI–HRI CROSS IDENTIFICATIONS

Source	Sequence No.	Detection No.[a]	α(1950)	δ(1950)
1H	H4481	1	0h37m30s.3	40°33′39″
2H	H4480	3	0 39 31.6	40 44 49
4H	H579	20	0 39 38.8	40 59 10
5H	H7066	2	0 39 46.8	41 0 25
6H	H579	10	0 39 50.6	41 0 21
7H	H7066	5	0 39 54.3	40 59 38
	H4479	15	0 39 54.3	40 59 40
	H579	14	0 39 54.5	40 59 40
8H	H4479	12	0 40 3.0	41 0 06
9H	H579	21	0 40 4.3	40 58 57
	H4479	24	0 40 4.4	40 58 58
10H	H4479	4	0 40 8.2	41 2 31
11H	H579	19	0 40 8.3	40 59 16
	H4479	20	0 40 8.3	40 59 17
12H	H579	15	0 40 10.6	40 59 39
	H4479	17	0 40 10.7	40 59 40
13H	H579	25	0 40 17.5	40 58 11
14H	H579	24	0 40 26.2	40 58 27
	H4479	26	0 40 26.2	40 58 28
15H	H4485	3	0 41 44.8	41 5 14
16H[b]	H4483	1	0 42 54.9	41 51 42
17H	H4484	1	0 43 0.5	41 23 22

[a] This is the identification number of the detection within the observing sequence as provided by the Final Data Processing.
[b] This detection shows variability.

$V_{\rm eff} = V_0/[2(2)^{1/2}]$, where V_0 is twice the amplitude of the sinusoid. $V_{\rm eff}(\Delta t)$ decreases as Δt increases beyond τ, thus allowing the determination of τ.

We have applied this method to the entire time span of each observation and for all of the selected sources and, in one case (source 4I; see next section for details), to individual continuous data segments. Our overall analysis was confined to time scales up to $\sim 10^5$ s and in any case shorter than individual observations. However, we have analyzed in further detail the variable sources, exploring their possible periodicity and comparing also the average count rates in different observations. In order to give information as complete as possible on these variable sources, in this second phase we have also included those detections of the variable sources yielding fewer than 60 counts.

TABLE 4

IPC–HRI CROSS IDENTIFICATIONS

IPC Source	HRI Source
4I..........	2H
6I..........	4H
10I..........	5H, 6H, 7H, 8H, 9H, 11H, 12H
12I..........	8H, 10H, 12H
15I..........	12H, 13H, 14H
24I..........	15H
25I..........	16H

Periodic variability was first explored by fitting the data to a model light curve characterized by alternating on and off states with five free parameters: amplitude, period, duration of the off phase, duration of the turn-on (symmetrical to the turn-off phase), and phase shift, as in Peres *et al.* (1989). In the following we shall refer to this as the "trapezoidal model." We have explored the space of time parameters initially using a grid of equally spaced periods, and then refining the grid around the local χ^2 minima. The amplitude and mean intensity which minimize χ^2 are computed analytically after the time parameters have been fixed.

We have also fitted the data with a sinusoidal model light curve characterized by four parameters: amplitude, period, time shift, and mean intensity. The parameter space was explored as for the previous fitting. Confidence contours of the period, of the time shift, and of the amplitude are computed according to Avni (1976).

Taking advantage of the moderate spectral resolution of the IPC, we have conducted our analysis in the broad band (0.2–3.5 keV) and in two narrower energy bands defined as the soft (0.2–0.8 keV) and the hard (0.8–3.5 keV) energy bands.

The standard background subtraction and instrumental corrections of the Final Data Processing (i.e., for vignetting, point spread function, and instrumental dead time were applied in deriving the count rates reported in the light curves. The possible effects of background variations during the observations are discussed below.

III. RESULTS

Two out of all sources analyzed are variable. Both sources are outside the crowded nuclear region and have been detected in more than one observation (Figs. 1*a* and 1*b*). Table 5 reports the identification of the two variable sources, the IPC X-ray luminosity (computed assuming a power law spectrum with a photon index of 1.5, a hydrogen column density of 3×10^{20} cm^{-2} [Fabbiano, Trinchieri, and van Speybroeck 1987], and a distance of 730 kpc), the observations and the energy bands in which variability was detected with the $\bar{\chi}^2$ method, the number of counts (including background) used in the analysis, the significance of variability, its effective amplitude, and its time scale.

A detailed analysis, presented below along with the results for individual sources, has ruled out the possibility that the variability originates from the background, in spite of its significant contribution to the counts within any source cell. The background was analyzed within an annulus centered on the field center, with inner and outer radii of 8′ and 15′, respectively, and excluding the sources thereby detected. Because of its significant contribution, however, the background signal dilutes the variability of the sources, making its detection harder and its estimated amplitude smaller. We have not corrected for this effect when quoting the amplitude (or upper bounds) of variability, but in § IV we present an extensive analysis on the chances of detecting variability for two specific models of source variability, considering also the influence of background.

Below we discuss the results for the two variable sources.

a) Source 4I

This source was in the field of view of four IPC (I574, I5021, I4490, and I573) and four HRI (H4480, H579, H4479, and H7066) observations (see Figs. 1*a* and 1*b*). The first two IPC observations yielded 1122 and 201 counts, respectively, while

TABLE 5

VARIABLE SOURCES

SOURCE	Log L_x[a] (ergs s^{-1})	Sequence Number	VARIABILITY ($\bar{\chi}^2$ method) Energy Band (keV)	Counts	Significance (%)	Effective Amplitude	Time Scale (s)
4I	37.6	I574	0.8–3.5	806	99.92	$16 \pm 3\%$	~ 6000
25I–16H	37.2	I575	0.2–3.5	613	99.84	$14 \pm 2\%$	>10000
		H4483	0.15–3.5	52	99.89	$40 \pm 6\%$	>7000

[a] L_x is from IPC observations.

in H4480 the source was detected with 51 counts. In I4490 the source was occulted by the detector window support structure and in all of the other observations the source was at the boundary or outside the field of view and was not detected; as mentioned in § II, I573 has been discarded. We have detected variability only during sequence I574, and only in the hard energy band, with a significance of 99.92%, a time scale of ~ 6000 s, and an effective amplitude of $16 \pm 3\%$ (see Table 5). In Figure 2 we show the light curve in I574 for the hard energy band. Each data point represents the average count rate in a single continuous data segment.

The analysis of the background photons (3092), collected from an area much larger than the source photon collection cell, yields no significant variability. The amplitude of variability with 6000 s binning (the time scale of variability of the source) is $\sim 4\%$ with a significance of only 90%.

The other two useful observations, I5021 and H4480, have fewer counts than I574 (in particular the net observing time of I5021 is $\sim \frac{1}{5}$ that of I574) and therefore detection of variability is much more unlikely. The upper limits on the amplitude of variability in these two observations are indeed consistent with the variablity detected in I574. We have also compared the flux in the two IPC observations, for any of the three energy bands, and found no significant change.

This source was identified with a globular cluster by C84. X-ray sources in globular clusters with luminosities in the range 10^{37}–10^{38} ergs s^{-1}, as observed for this source, are typically low-mass X-ray binaries, henceforth LMXRB (Bradt and McClintock 1983 and references therein). Their X-ray light

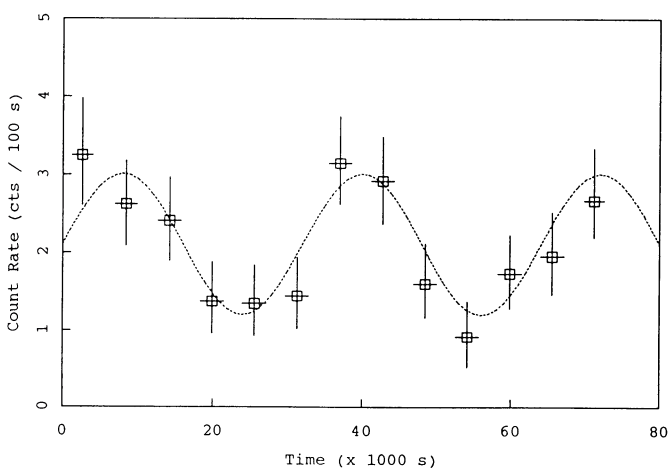

FIG. 2.—IPC light curve (hard-energy band) of source 4I. The horizontal bars yield the time span over which each count rate was averaged, and the vertical error bars account only for statistical error. The count rates are corrected for instrumental effects and background. The dashed line is the best fit to the sinusoid plus a constant value model light curve.

curves are usually variable and often show periodic features (Parmar and White 1988). In particular the light curve of Cyg X-3 (Becklin *et al.* 1973), a Galactic LMXRB with periodic modulations in X-rays, resembles the light curve of source 4I. Extending the analogy also to a possible periodicity, we infer that the data could show two cycles, with low phases at $t \sim 2.5 \times 10^4$ s and $t \sim 5 \times 10^4$ s and high phases at $t = 4 \times 10^4$ s and, maybe, at the beginning and at the end of the observation.

We have searched for periodicity, with the method described in § II, in a range of periods between 2×10^4 s and 2.02×10^5 s. The fitting to the trapezoidal model yielded a minimum reduced χ^2 of 1.38 with 8 degrees of freedom. We have however preferred to turn to the sinusoidal modulation plus a constant for the following reasons: the source does not seem to turn off during minima, trapezoidal modulations have never been observed in Galactic LMXRBs, and the second model has four instead of five free parameters. The fitting yielded a reduced χ^2 of 0.57 with 9 degrees of freedom. The probability of exceeding by chance this value of χ^2, under the null hypothesis of a periodic source with the estimated parameters, is 80%; the analogous probability of exceeding the χ^2 value obtained under the null hypothesis of a constant source is 0.08%. Therefore the periodic model cannot be rejected at 99.73% significance level and it significantly improves the fit with respect to a constant light curve governed by Poisson noise.

The parameters which minimize the χ^2 are: period = 32,500 s, amplitude = 0.89×10^{-2} counts s^{-1}, mean intensity 1.99×10^{-2} counts s^{-1}, time shift since the beginning of observation, -1000 s. In Figure 2, we show the best fit along with the X-ray light curve. We note that this fitting supports minima consistent with a nonzero flux, a typical feature of low-mass binaries. The 68% and 90% confidence contours, calculated according to Avni (1976), are plotted both in the period-amplitude plane (Fig. 3*a*), and in the period-timeshift plane (Fig. 3*b*), and show a relatively narrow range of periods (~ 3000 s around the best-fit value), of amplitude ($\sim 2.5 \times 10^{-2}$ counts s^{-1}), and of time shift (~ 3000 s).

Since LMXRBs are often X-ray bursters, we have also studied the variability within each continuous data section of the two IPC observations, checking for variability at bin sizes in the range 150–800 s. We found none. The HRI observation yields too few counts to allow a valid application of this analysis.

b) Source 25I

This source was well within the field of view of one IPC (I575) and one HRI (H4483) observation and was detected in both, with 613 and 52 counts, respectively. We detected variability during the IPC observation in the broad energy band, with a significance of 99.84%, a time scale greater than 10,000 s and an effective amplitude of $14 \pm 2\%$. The light curve in this

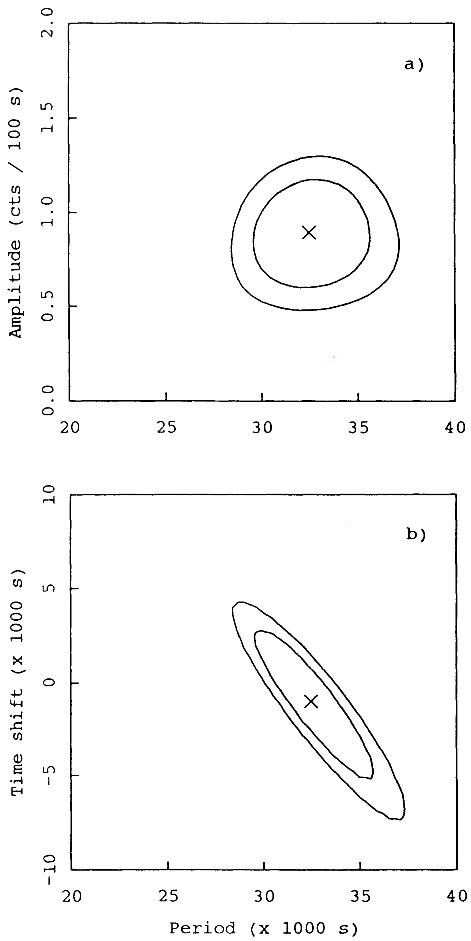

FIG. 3.—The 68% (*inner*) and 90% (*outer*) confidence contours for the fitting of the I574 light curve of source 4I determined as in Avni (1976). The data pertain to the hard-energy band (0.8–3.5 keV), and the model light curve consists of a sinusoid plus a constant value. Panel (*a*) reports the plane of interesting parameters period-amplitude and panel (*b*) the plane period-time shift. The cross marks the values of absolute minimum reduced χ^2 (0.57, 9 degrees of freedom), corresponding to a period of 32,500 s, a time shift of -1000 s since the beginning of the observation, amplitude of 0.89×10^{-2} counts s^{-1}, and a constant value of 1.99×10^{-2} counts s^{-1} (cf. Fig. 2).

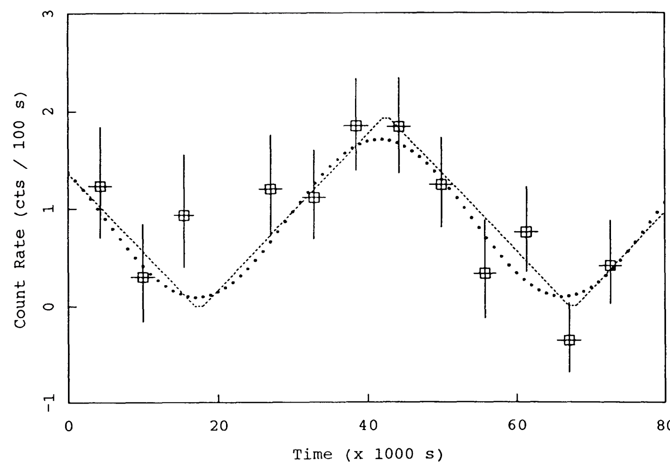

FIG. 4.—Light curve of source 25I in the broad energy band. Error bars and count rate corrections as for Fig. 2. The dashed and dotted lines are the best fit to the trapezoid and to the sinusoid plus a constant value model light curve, respectively.

band, derived as for Figure 2, is shown in Figure 4. It presents two low phases at $t \sim 10{,}000$ s and $t \sim 65{,}000$ s, compatible with background emission alone.

The analysis of the background (6263 photons) of this IPC observation taken from an area much larger than the source photon collecting cell shows that it is indeed variable with an effective amplitude of $\sim 12\%$ but at a time scale of ~ 500 s. The amplitude of variability decreases monotonously with increasing binning size and is only 3% at $\sim 10{,}000$ s, compatible with statistical fluctuations. As a further check, three sources detected in the same observation (excluded by our selection), one of which had approximately the same number of counts as 25I, show no variability.

Despite the low number of counts (52), we also have analyzed H4483 which, as reported in Table 1, is made up of two segments taken a few months apart and lasting $\sim 12{,}000$ and $\sim 17{,}000$ s respectively (see Table 1). The first segment could not be analyzed because it contained too few counts (12). No variability was detected during the second data segment; given the upper limit of variability and the slightly different bandpass of the HRI, this result does not contradict the variability detected during the IPC observation.

We also have explored the variations within the whole sequence, therefore analyzing also the long-term (time scale $\gg 10^5$ s) variability of this source. In the particular case of H4483, the two data segments, though equivalent to two different observations, have the same pointing direction and roll angle, thus eliminating the calibration problems arising when comparing different observations. Therefore we have applied the $\bar{\chi}^2$ method to the whole sequence, detecting variability significant at 99.89% with a time scale greater than 7000 s and an effective amplitude of $40 \pm 6\%$. Since the first segment yields a very small contribution to the statistics and the second segment is constant, the variability could be due to significant differences of average count rate between the two data segments. In fact, the count rates during the two data segments are $(0.98 \pm 0.28) \times 10^{-3}$ and $(2.40 \pm 0.38) \times 10^{-3}$. Under the hypothesis that the count rate is constant during each of the two segments of the observation and equal to its mean value in that segment, we derive that the $\bar{\chi}^2$ method would detect an effective amplitude of variability of 44%, a value in good agreement with the amplitude effectively found. It is hence plausible to ascribe the variability detected in the overall observation mostly to the change of count rate between the two segments. Upper and lower limits to the time scale of variability are, therefore, 5 months, the total time span of the observation, and 7000 s, as obtained with the $\bar{\chi}^2$ method.

This source had been identified with an OB star with blue apparent magnitude $m_b = 20.5$ (cf. C84). The low phases of the IPC light curve (Fig. 4), compatible with no emission at all from the source, are analogous to those of compact intense Galactic X-ray sources and of source X-7 of M33 (Peres *et al.* 1989). These features and the X-ray luminosity ($\sim 10^{37}$ ergs s^{-1}) suggest that this source is a massive compact X-ray binary, henceforth MXRB. In this case, the variability could be either periodic, because of orbital modulation, or erratic and due to an intrinsic variation of the X-ray luminosity of the compact X-ray source, as observed in Galactic compact X-ray binaries (Schreier *et al.* 1972). We have applied the analysis of periodicity, described in § II, to a range of periods between 2×10^4 and 2.02×10^5 s. First we fitted the observations with

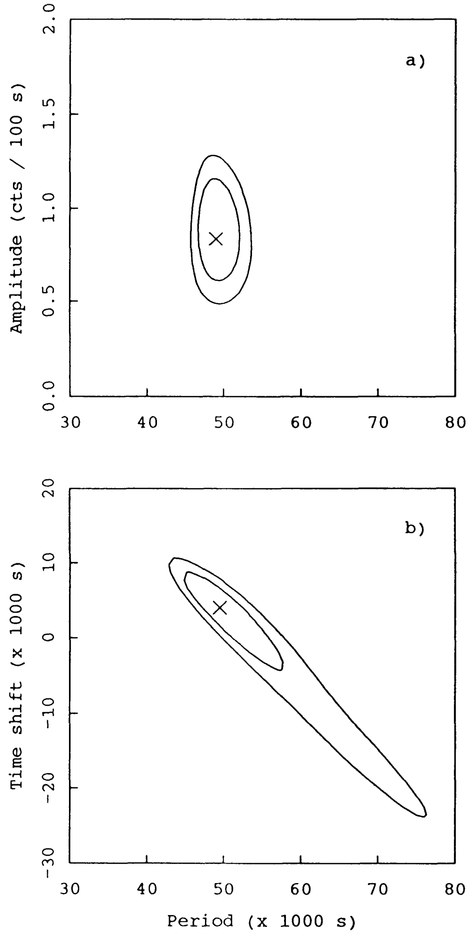

FIG. 5.—The 68% (*inner*) and 90% (*outer*) confidence contours for the fitting of the I575 light curve of source 25I determined as in Avni (1976). The data pertain to the broad energy band (0.2–3.5 keV), and the model light curve consists of a sinusoid plus a constant value. Panel (*a*) reports the plane of interesting parameters period-amplitude and panel (*b*) the plane period-time shift. The cross marks the values of absolute minimum reduced χ^2 (0.89, 8 degrees of freedom), corresponding to a period of 49,500 s, a time shift of 4000 s since the beginning of the observation, amplitude of 0.83×10^{-2} counts s^{-1}, and a constant value of 0.97×10^{-2} counts s^{-1} (cf. Fig. 4).

the trapezoidal model (dashed line in Fig. 4) obtaining a minimum reduced χ^2 of 0.85 with 7 degrees of freedom. Although this model is a realistic one for this kind of source, we obtained the strange result that on and off phases lasted both 1000 s, 1/50 of the period, whereas the virtual totality of the light curve would be made up by the decay and rise phase, i.e., the light curve is a symmetric triangular modulation with minima consistent with zero flux. We then turned to the sinusoidal plus constant model light curve (dotted line in Fig. 4). We obtained a reduced χ^2 of 0.89 with 8 degrees of freedom. The probability of exceeding by chance this χ^2 value under the null hypothesis of the periodic model is greater than 50%. We have derived a period $T = 49{,}500$ s, an amplitude of -0.83×10^{-2} counts per s,[1] a constant value of 0.97×10^{-2} counts s^{-1}, and a time shift of 4000 s. We show in Figure 5*a* and 5*b*, the 68% and 90% confidence contours for pairs of the fitted parameters. Although the fit is good, the period is poorly constrained, as shown by the confidence contours reported in Figure 5*b*, because it is comparable to the whole time span of the observation, i.e., we are observing a little more than a single period. Therefore a period of 76,000 s is still compatible with the data and the assumed model light curve at a 90% confidence level, although the period is limited to less than 57,000 s at the 68% confidence level.

[1] The negative value indicates an additional shift of half a phase. In all of the following and in the figures we use the absolute value of the amplitude.

c) *Upper Limits on Variability of Other Sources*

In Tables 6 and 7 we report, for the IPC and the HRI, respectively, the upper limits on the variability of all the sources analyzed: we give the sequence number, the detection number, the number of counts, the explored range of binning sizes, the corresponding range of upper limits to the amplitude of variability computed at the 99.73% level, and the effective variability; in the last two columns we provide the effective amplitude which the same method would detect for two different models of variability, as described in detail in § IV*d*. The upper limits depend on the total number of detected counts and on the binning size explored. The count rate determines the minimum bin size that can be explored and the maximum is constrained by the observation length or, in most cases, by the observational gaps. In § IV we further discuss the chances of detecting variability in our sample.

Our analysis has been mainly confined to variability within individual observations; possible long-term variability has therefore escaped detection. A systematic long-term variability analysis, on the other hand, will require an accurate preliminary morphological analysis (cf. Trinchieri *et al.* 1990) of the new data obtained with the Final Data Processing.

IV. DISCUSSION AND CONCLUSION

We have studied the variability of the X-ray sources in M31. Two sources (4I and 25I) are variable above the 99.73% threshold of significance.

a) *Source 4I*

Source 4I was identified with a globular cluster by C84. On the basis of the parameters of variability, the shape of the light curve, and the optical identification with a globular cluster, we have suggested that the source 4I is an LMXRB. The variability is detected in the hard energy band but neither in the soft nor in the broad energy band. A variability in the soft band scaled proportionally to the count rate of the hard band would not be detectable, but this conjectured variability over the entire bandwidth would be easily detectable in the broad-band analysis. All this suggests that the variability in the soft band, if any, is rather small.

The χ^2 fitting to a sinusoidal modulation is more appropriate than that to a trapezoidal modulation: We find that the source is not off during minima and that the light curve and the period value are fairly consistent with those of some well-studied Galactic LMXRBs (Parmar and White 1988); the confidence level is satisfactory. We find for source 4I a period of $\sim 3.25 \times 10^4$ s. Assuming 2 $M_\odot$ as the total mass of the system and a circular orbit with this period, we infer 2×10^{11} cm as the separation between the two components of the system.

The sinusoidal modulation of the light curve supports the idea that this could be the first detection of periodicity of an LMXRB in an outer galaxy. Although we cannot exclude the possibility that models of variability other than periodic ones can equally well fit the data, the resemblance of the X-ray light curve of this source with that of Galactic LMXRBs cannot be dismissed lightly.

b) *Source 25I*

Source 25I was identified with a blue star by C84. The low phases, consistent with zero count rate, of its light curve and the optical identification with a blue star suggest an MXRB.

This source has been found to be significantly variable in two independent observations. The χ^2 fitting of the light curve to the trapezoidal light curve and to the sinusoid has yielded a period of 49,500 s. Despite the acceptable χ^2 value, the test yields a poor upper constraint on the period and makes evidence of periodicity rather unconvincing. The HRI data, because of their poor statistics, do not help much in this respect. Furthermore the light curve is unusual for MXRBs, but on the other hand, the minima are consistent with zero flux, a feature typical of eclipsing MXRBs.

There are a few options still compatible with observations

TABLE 6A

Upper Limits (IPC Hard Band) on the Amplitude of Variability

Sequence No.	Source No.	Counts	Bin Sizes (s)	Amplitude[a] (%)	Amplitude[b] % (mod. 1)	Amplitude[b] % (mod. 2)
I574......	1	186	1200–9200	36–25	<3	<1
I574......	4	1562	200–9100	19–9	77	24
I574......	5[c]	806	400–9200	...	55	17
I574......	6	386	600–9200	29–17	5	2
I574......	7	2959	100–9150	16–6	88	28
I574......	9	450	600–9200	27–16	18	6
I574......	11	470	600–9200	26–16	22	7
I574......	12	9664	30–9150	12–3	~95	~30
I574......	13	1323	200–9100	20–9	72	23
I574......	14	3916	60–9140	16–5	91	29
I574......	15	607	400–9200	25–14	40	13
I574......	16	1222	200–9100	21–10	70	22
I574......	17	2385	100–9150	18–7	85	27
I574......	18	555	400–9200	26–15	34	11
I574......	20	555	400–9200	26–15	34	11
I574......	21	908	400–9200	21–11	60	19
I574......	23	504	600–9200	25–15	28	9
I575......	13	314	700–8200	31–19	31	10
I4490.....	3	537	200–2800	24–15	82	26
I4490.....	4	132	600–2800	38–28	26	8
I4490.....	6	180	400–2800	36–24	46	14
I4490.....	7	2464	40–2780	17–6	96	30
I4490.....	8	294	300–2800	30–20	67	21
I4490.....	9	503	200–2800	25–15	81	26
I4490.....	10	348	200–2800	30–18	72	23
I4490.....	11	155	600–2800	35–26	37	12
I4490.....	12	177	400–2800	36–24	45	14
I4490.....	14	310	300–2800	29–19	69	22
I4490.....	15	275	400–2800	29–19	65	20
I4490.....	16	148	600–2800	36–26	34	11
I4490.....	17	184	400–2800	35–23	47	15
I4490.....	18	153	600–2800	36–26	37	11
I4490.....	19	187	400–2800	35–23	48	15
I5021.....	1	133	400–2000	39–30	68	21
I5021.....	8	125	400–2000	40–31	65	21
I5021.....	11	68	800–2000	48–42	36	12

[a] Upper limits on the amplitude of variability.
[b] § IV*d* for its definition.
[c] Variable detection (see also Table 5).

TABLE 6B

Upper Limits (IPC Soft Band) on the Amplitude of Variability

Sequence No.	Source No.	Counts	Bin Sizes (s)	Amplitude[a] (%)	Amplitude[b] % (Model 1)	Amplitude[b] % (Model 2)
I574......	5	316	800–9200	30–19	14	5
I574......	12	4079	60–9150	16–5	93	30
I574......	13	604	400–9100	26–14	55	17
I574......	21	450	600–9200	27–16	40	13
I575......	13	299	700–8200	31–20	29	9
I4490.....	7	1060	80–2780	22–10	93	30
I4490.....	9	91	800–2800	44–36	22	7
I4490.....	15	128	600–2800	39–28	44	14
I4490.....	19	80	1000–2800	44–36	12	4

[a] Upper limits on the amplitude of variability.
[b] See § IV*d* for its definition.

TABLE 6C

UPPER LIMITS (IPC BROAD-BAND) ON THE AMPLITUDE OF VARIABILITY

Sequence No.	Source No.	Counts	Bin Sizes (s)	Amplitude[a] (%)	Amplitude[b] % (Model 1)	Amplitude[b] % (Model 2)
I574......	3	677	400–9100	24–13	13	4
I574......	4	2107	150–9150	17–8	72	23
I574......	5	1122	200–9100	22–10	47	15
I574......	6	611	400–9100	26–14	4	1
I574......	7	4046	60–9140	16–5	85	27
I574......	9	763	300–9100	24–13	23	7
I574......	12	13743	20–9150	11–3	>95	>30
I574......	13	1927	150–9150	18–8	69	22
I574......	15	968	300–9100	22–11	39	12
I574......	16	1915	150–9150	18–8	69	22
I574......	17	3502	80–9140	16–5	83	26
I574......	18	836	300–9100	23–12	29	9
I574......	19	1469	150–9150	21–9	60	19
I574......	20	852	300–9100	23–12	31	10
I574......	21	1358	200–9100	20–9	57	18
I574......	23	830	300–9100	23–12	29	9
I575......	13[c]	613	400–8200	...	30	10
I4490.....	3	742	100–2800	24–13	80	25
I4490.....	6	242	300–2800	33–22	40	13
I4490.....	7	3524	20–2780	16–5	96	30
I4490.....	8	430	200–2800	27–17	66	21
I4490.....	9	594	150–2800	25–14	76	24
I4490.....	11	240	300–2800	33–22	40	13
I4490.....	12	268	300–2800	31–21	46	15
I4490.....	14	435	200–2800	27–16	67	21
I4490.....	16	215	400–2800	33–23	33	10
I4490.....	17	288	300–2800	30–20	50	16
I4490.....	18	214	400–2800	33–23	33	10
I4490.....	19	267	300–2800	32–21	46	15
I5021.....	1	201	300–2000	34–24	61	19
I5021.....	8	178	300–2000	36–26	56	18
I5021.....	11	112	500–2000	41–33	29	9

[a] Upper limits on the amplitude of variability.
[b] See § IV*d* for its definition.
[c] Variable detection (see also Table 5).

TABLE 7

UPPER LIMITS (HRI) ON THE AMPLITUDE OF VARIABILITY

Sequence No.	Detection No.	Counts	Bin Sizes (s)	Amplitude[a] (%)	Amplitude[b] % (Model 1)	Amplitude[b] % (Model 2)
H579......	10	106	2000–7000	39–31	92	29
H579......	14	446	400–7200	28–16	98	31
H579......	15	83	2500–7000	43–35	90	28
H579......	19	203	1000–7200	34–24	96	30
H579......	20	100	2000–7000	40–32	92	29
H579......	21	105	2000–7000	39–32	92	29
H579......	24	75	2500–7000	45–37	89	28
H579......	25	64	3000–7000	47–40	87	28
H4479.....	4	64	2500–6500	48–40	90	28
H4479.....	12	82	2000–6500	44–35	92	29
H4479.....	15	404	400–6500	29–17	98	31
H4479.....	17	96	1800–6600	43–35	93	29
H4479.....	20	144	1200–6400	38–27	95	30
H4479.....	24	75	2500–6500	44–37	91	29
H4479.....	26	67	2500–6500	47–39	90	28
H4480.....	3[c]	51	3200–6800	53–47	84	30
H4480.....	6	77	2200–6800	47–39	94	30
H4481.....	1	102	600–2400	43–34	98	31
H4484.....	1	151	400–2400	39–29	99	31
H4486[d]....	...	...	...	...	...	...
H4485.....	3	66	2300–6200	50–42	93	29
H4483.....	1[c]	52	4000–7000	...	85	27
H7066.....	2	213	300–2600	33–21	98	31
H7066.....	5	66	950–2600	47–39	93	30

[a] Upper limits on the amplitude of variability.
[b] See § IV*d*, for its definition.
[c] This source was included because variable in the IPC.
[d] None of the sources detected in this sequence was selected for the analysis.

and which cannot be excluded by our analysis. Among them we can mention that the source might be periodic with a much longer period (cf. discussion on Fig. 5*b*), especially because the period we find is smaller than that of any MXRB known, and we might just be detecting an high-low transition, occurring after $t \sim 40{,}000$ s (cf. Fig. 4). We might also be detecting just a transient phase of the source. On the other hand, one could think that the light curve we find is indeed appropriate and the source, is, by chance, angularly close to a blue star but physically unrelated to it. Far from conclusive, the above arguments point to the need for future more detailed observations of this source, for instance using the *ROSAT* satellite, taking into account the requirements of studies of variability.

c) General Methodology

Given the large number of tests and the relatively small number of variable sources, one might wonder whether they arise as statistical fluctuations of a set of constants. In this respect an overview of our methodology, the same used by Peres *et al.* (1989), will clarify the physical reliability of our findings.

We initially selected *Einstein* detections on the basis of a few criteria: count statistics higher than a threshold, no possible influence from occulting structures in the detector, low chances of arising from statistical fluctuations of local background, etc.

We then analyzed these detections with the "$\bar{\chi}^2$ method," i.e. we further screened them, selecting only those showing variability which could arise by chance from a constant source only in 0.27% of the cases. This could still leave room for doubting whether the variable sources are simply statistical fluctuation.

However, we are screening out purely statistical fluctuations. We have searched these sources for periodicity, finding for 4I a good agreement with the light curve one would expect from an LMXRB, and for 25I a fair agreement with the picture of an MXRB. The fitting with periodic light curves yields an improvement of significance with respect to the other, purely stochastic model, and, on the other hand, the optical identifications by C84 provide further support to this picture. Furthermore, 25I was found variable in two independent detections and chances of such statistical fluctuations in two detections are extremely low.

d) Upper Limits and Chances of Detecting Variability in Our Sample

On the other hand, most of the sources detectable in M31 should be highly variable, and instead the fraction of variable sources is, at first glance, small. The upper limits on detectable *effective* variability, presented in Tables 6 and 7, provide a first evidence that this result is not surprising and points to the need for better observations.

As a further check we have estimated also the number of variable sources, similar to the two we have found, that we should expect to detect in our sample using the $\bar{\chi}^2$ method. We have taken into account the known features of the brightest X-ray Galactic sources and the number and features of IPC detections in M31. We shall show that, even overestimating the expected number of detectable variable sources, our findings are consistent with expectations.

On the basis of the X-ray luminosity of Galactic sources, of the detection threshold at the distance of M31, and of the work by C84 we assume that our sample consists completely of MXRBs, LMXRBs, and foreground sources (henceforth FGs), and neglect the possibility of other kinds of sources, including spurious ones.

C84 provide the identifications of some sources. As for the dubious identification, or whenever the IPC source includes several distinct HRI sources, we have chosen (cf. Table 2) the most reliable one among those provided by C84. We take that sources identified with globular clusters are LMXRBs, sources identified with blue stars are MXRBs, and assume that all sources not identified by C84 are LMXRBs, because they are not identified either with a blue star in M31 or a FG, both optically bright and therefore easily detectable counterparts.

Our sample includes, because of the most recent processing, some sources not reported by C84. We assume that the relative fractions of MXRBs, LMXRBs and FGs among these new and unidentified sources are the same as among the rest of the sample. We then assign artificial identifications, also reported in Table 2, to each of the new detections through a Monte Carlo simulation.

As for the MXRBs we then assume that they vary periodically according to a square light curve with on and off states of equal duration, the off states yielding no detectable flux. This model is defined as Model 1 in the tables. We have assumed that all of the MXRBs in our sample are variable, with the same period distribution of Galactic MXRBs of known period (Bradt and McClintock 1983).

As for the LMXRBs we have assumed that their light curve consists of a sinusoidal plus a constant X-ray flux, with the same parameters obtained for source 4I. This model is defined as Model 2 in the tables. It is worth noting that LMXRBs exhibit two other kinds of variability, periodic dips and bursts, which however do not last long enough to be detected with our data. We make the further simplifying assumption that the period is always shorter than the time span of the observation being considered. Although this is not always true for Galactic LMXRBs, this assumption increases the probability of detecting variability and therefore overestimates the expected number. About $\frac{1}{5}$ of the Galactic LMXRBs, virtually all of the well-observed ones, are periodic and about 1/3 of them exhibit sinusoidal modulation (Parmar and White 1988). We assume that all LMXRBs are periodic, the smaller fraction detected in our Galaxy being due only to the lack of detailed observations, i.e., that whenever an LMXRB is observed sufficiently well some kind of variability must be detected, and that $\frac{1}{3}$ of the LMXRBs in our sample have sinusoidally modulated light curves.

FGs will not be considered in the following analysis, because we are interested only in the sample of M31 sources.

For each detection and using the mean field background, we computed the effective variability which would be detectable using the $\bar{\chi}^2$ method for each variability model; the relative results are reported in Table 6 and Table 7. Considering the three IPC energy bands, there are nine LMXRBs and 11 MXRBs in which we can potentially detect variability of the types of the two models. They indeed include 4I and 25I. Given the typical time scales of variability which we are considering, the threshold is determined by the largest bin size explored.

The fraction of the LMXRBs expected to have a detectable sinusoidal modulation is $\frac{1}{3}$ of the total, yielding an expected number of variability detections of three, consistent with the one found, especially considering that the assumptions tend to overestimate the expected number.

For the MXRBs the computation is not so straightforward because their periods tend to be longer than the time span of the observations. We have therefore estimated the probability of the occurrence which would provide variability, i.e., finding an on-off or off-on transition in the time span of each observation, for any of the periods observed in galactic MXRBs and assigning equal probability, 1/12, to all of the 12 MXRB periods used (drawn from Bradt and McClintock 1983). The probability of observing variability in a selected detection, for a given period, is the product of the probability of observing a transition times the probability of that particular period (1/12). We then compute the expected number of variability detections, which turns out to be 2.4, again consistent with one. Also here we note that the hypotheses adopted tend to give an overestimate of the expected number. In particular, we note that (*a*) a square modulation with 50% duty cycle yields the highest chances of detecting variability; (*b*) the assumption that the duty cycle is 50% and that the whole sample of observed MXRBs obeys our variability model is unrealistic, because the off states in all known MXRBs are much shorter; (*c*) even if the duty cycle is 50%, real observations, if shorter than the period, yield a 50% duty cycle only if the transition occurs exactly in the middle of the observation time span. For all of these reasons, according to equation [3.13] of Collura *et al.* (1987) the $\bar{\chi}^2$ should yield a smaller effective amplitude of variability and therefore a less observable one. Also the assumption that all of the MXRBs are variable may be too conservative.

Many of the strongest IPC sources are, on the other hand, the unresolved combination of two or more HRI sources; if only one source is variable, the detection of its variability is much less likely than for a single source.

The analogous estimate of the expected number of variability detections in the HRI data leads to similar results.

We have proved that our findings are consistent with reasonable expectations. As for the variable sources, the picture could be considerably improved: more observations or longer ones undoubtedly would have provided better information on features such as amplitude and period of variability. Longer, repeated and high-resolution observations should also detect more variable sources in M31. In this respect the results on the variable sources, as well as the upper limits on detectable variability presented in Tables 6 and 7 can help in planning both the pointing and the duration of the observations to be performed in future X-ray missions.

We thank G. Fabbiano for her help, S. Hazelton for the first data reduction, G. Micela, S. Sciortino, and G. S. Vaiana for useful discussions and suggestions, S. Serio for a critical revision of the manuscript, and an anonymous referee for having considerably improved the quality of the presentation. G. P. acknowledges the CNR-NATO Senior Fellowship 217.18 and 217.19; F. R. acknowledges partial support by the Sicilian Consiglio Regionale delle Ricerche Nucleari e della Struttura della Materia. This work was supported in part by the Ministero per la Pubblica Istruzione and by the Consiglio Nazionale delle Ricerche.

REFERENCES

Avni, Y. 1976, *Ap. J.*, **210**, 642.
Becklin, E. E., Neugebauer, G., Hawkins, F. J., Mason, K. O., Sandford, P. W., Matthews, K., and Wynn-Williams, C. G. 1973, *Nature*, **245**, 302.
Bradt, H. V. D., and McClintock, J. E. 1983, *Ann. Rev. Astr. Ap.*, **21**, 13.
Collura, A., Maggio, A., Sciortino, S., Serio, S., Vaiana, G. S., and Rosner, R. 1987, *Ap. J.*, **315**, 340.
Crampton, D., Cowley, A. P., Hutchings, J. B., Schade, D. J., and van Speybroeck, L. P. 1984, *Ap. J.*, **284**, 663 (C84).
Fabbiano, G., Trinchieri, G., and van Speybroeck, L. P. 1987, *Ap. J.*, **316**, 127.
Giacconi, R., *et al.* 1979, *Ap. J.*, **230**, 540.
Harnden, F. R., Jr., Fabricant, D. G., Harris, D. E., and Schwarz, J. 1984, *SAO Spec. Rept.* No. 393.
Harnden, F. R., Jr., Vaiana, G. S., Sciortino, S., Micela, G., Maggio, A., Schmitt, J. H. M. M., and Rosner, R. 1989, in preparation.
Ilovaisky, S. A., 1985, *Interacting Binaries*, ed. P. P. Eggleton and J. E. Pringle, (Dordrecht: Reidel), p. 205.
Parmar, A. N., and White, N. E. 1988, *Mem. Soc. Astr. Italiana*, **59**, 147.
Peres, G., Reale, F., Collura, A., and Fabbiano, G. 1989, *Ap. J.*, **336**, 140.
Schreier, E., Levinson, R., Gursky, H., Kellog, E., Tananbaum, H., and Giacconi, R. 1972, *Ap. J.* (*Letters*), **172**, L79.
Schreier, E. J., Swartz, K., Giacconi, R., Fabbiano, G., and Morin, J. 1976, *Ap. J.*, **204**, 539.
Tananbaum, H., Gursky, H., Kellog, E. M., Levinson, R., Schreier, E., and Giacconi, R. 1972, *Ap. J.* (*Letters*), **174**, L143.
Trinchieri, G., *et al.* 1990, in preparation.
van Speybroeck, L. P., Epstein, A., Forman, W., Giacconi, R., Jones, C., Liller, W., and Smarr, L. 1979, *Ap. J.* (*Letters*), **234**, L17.

ALFONSO COLLURA: Istituto per le Applicazioni Interdisciplinari della Fisica—Consiglio Nazionale delle Ricerche, Via Archirafi 36, 90123 Palermo, Italy.

GIOVANNI PERES: Osservatorio Astrofisico di Catania, V. le A. Doria 6, 95125 Catania, Italy.

FABIO REALE: Osservatorio Astronomico, Palazzo dei Normanni, 90134 Palermo, Italy.